RESEARCH ARTICLE

Geospatial Patterns of Non-Melanoma Skin Cancer in Relation to Climate Changes in Iran

Michael Aryan Kya*

Abstract

   Objective: The purpose of this study is to examine the impact of climate change factors on the incidence of skin cancer in Iran. **Methods:** The statistical population for this study comprises skin cancer patients in Iran. All other data used in this research were extracted from Remote Sensing imagery, including Ultraviolet ray, Relative humidity, Cloud cover, incoming short-wave flux, elevation, and total hours of sunshine. Initially, spatial autocorrelation analysis and cluster patterns were calculated using General G and Moran's I indices. Subsequently, a Geographically Weighted Regression Model was used to establish a regression relationship between the climate change data and the detection and forecasting rate of skin cancer. Finally, the model's accuracy was evaluated by estimating the detection coefficient between the reality map and the forecasting map. **Results:** The study found that UV radiation and relative humidity exhibit the highest positive and negative correlation, respectively, with the skin cancer rate in Iran. Geostatistical analysis revealed a clustered spatial distribution of skin cancer rates, and the proposed GWR model demonstrated high accuracy in predicting the skin cancer rate. The results indicate the highest positive correlation (+0.51) for UV ray and the most negative correlation (-0.43) for relative humidity. The Geostatistical analysis reveals spatial autocorrelation, cluster patterns, and non-randomness of the data. **Conclusion:** The detection rate of skin cancer increases from north to south and from west to east.

   Keywords: Skin cancer- climate Change- spatial behavior- Iran

Introduction

   Malignant melanoma (MM) and Non-Melanoma Skin Cancer (NMSC) represent the two primary types of skin cancer. NMSCs consist of Basal Cell Carcinoma (BCC), Squamous Cell Carcinoma (SCC), and Bowen's disease. Both NMSC and MM show a concerning increase in incidence rates [1, 2]. In addition to various factors, such as family or personal history, a weakened immune system, and pale skin color, the prevalence of this disease also depends on environmental factors. Prolonged exposure to UV radiation is recognized as the most significant environmental risk factor for skin cancer [3-8]. Based on primary epidemiological evidence, solar radiation plays a crucial role in the development of skin cancer. Environmental studies further indicate that the prevalence of this cancer is linked to changes in latitude and altitude [9]. According to these studies, skin cancer rates tend to increase at lower latitudes and higher altitudes. Additionally, evidence suggests that outdoor activities, increased exposure to UV radiation, and total sunshine hours can also contribute to the incidence of skin cancer [10]. In this regard, various types of skin cancer are significantly linked to environmental conditions and the level of ultraviolet (UV) radiation exposure [11]. The

role of environmental components, including pollution, outdoor activities, radiation exposure, and climate changes, has been studied concerning skin cancer [12, 13]. Wheeler et al (2013), examined the correlation between skin cancer rates and three factors: Radon, Arsenic, and sunshine hours in England. They found no association between arsenic exposure and skin cancer. However, there were significant correlations observed between sunshine hours and Radon density with cancer rates; sunshine had a high correlation, while Radon had a medium correlation [14]. Correspondingly, Hu et al (2014), applied spatial analysis to predict high-risk neighborhoods for late-stage skin cancer in Florida. Their study revealed that Hispanic whites and residents of poor neighborhoods were more likely to be diagnosed with skin cancer [15].

   The recognition of epidemics holds great importance in public health, and understanding the geographical distribution of a disease is one of the most effective factors in this process. Since disease prevalence is related to the environment and climate, studying geographical conditions becomes essential [16, 17]. However, spatial data analysis for investigating epidemics often presents challenges, prompting public health experts to seek solutions. The use of maps was one of the initial methods for incorporating spatial analysis into epidemic investigations, and today,

*Department of Dentistry, School of Dentistry, Medical University, Tehran, Iran. *For Correspondence: mekheilaryan@gmail.com*

Michael Aryan Kya

Geographic Information Systems (GIS) serves as a powerful tool for decision-making in this field [18, 19].

The impact of climate change as an environmental factor on skin cancer has been the subject of study [20, 21]. Wright et al (2019), concluded that climate change could impact current incidence rates of skin cancer in several ways. These impacts are associated with shifts in meteorological variables, particularly air pollution, temperature, rainfall, and cloud cover, which all affect solar ultraviolet radiation (UVR) levels at the Earth's surface. While they emphasize more data are needed to fully understand these effects, it is likely that increasing air pollution could lead to cutaneous damage, thereby elevating the risk of skin cancer [22].

In Iran, skin cancer is among the most prevalent types of cancer, with the head and neck being the most affected areas [23, 24]. Additionally, skin cancer is reported to have a higher prevalence compared to other types of cancer, and Basal Cell Carcinoma (BCC) is the most common morphologic form of skin cancer in Iran [25, 26]. In this regard, the role of climate change in skin cancer in Iran has been overlooked. Furthermore, studies concerning environmental factors and skin cancer in Iran have primarily focused on single factors. Therefore, the purpose of this study is to map the spatial distribution of skin cancer in Iran, considering its spatial correlation with various climate change factors using Geographical Weighted Regression and Remote Sensing data.

Materials and Methods

Process of study

Figure 1 illustrates the steps taken in this study.

Area of study

Iran, spanning over 1.6 million square kilometers, is situated between 25°N to 29°N latitude and 44°E to 63°E longitude (Figure 2). As per the 2022 reports from the Statistical Center of Iran, the country's population is approximately 82,011,735. Geographically, Iran is classified as a semi-arid region. Figure 2 illustrates the study area.

Data

Based on existing evidence and previous studies mentioned earlier, it is evident that environmental and climatic conditions significantly influence the spatial distribution of skin cancer. Consequently, demographic data, disease information, and climate change parameters were utilized for mapping the spatial dispersion of skin cancer. The required information was obtained from various sources. Demographic data for the year 2022 was acquired from the Statistical Center of Iran. Similarly, information on skin cancer was gathered from the non-communicable diseases department of the Iran Tumor Bank for the same year. To mitigate the impact of population size on the results for both highly populated and low population cities, the data were adjusted to calculate the rate of skin cancer for each city using equation 1.

$$\text{Skin cancer rate} = \frac{number\ of\ cases\ within\ a\ defined\ time}{total\ population} \times 100000 \quad (1)$$

The rate of skin cancer for every 100,000 individuals was represented by the value of 100,000. The sunshine hours map was obtained from the Ministry of Energy. Climate change data were acquired through satellite imageries. Altitude data was extracted from DEM maps sourced from SRTM images with a spatial resolution of 90 meters. In line with the increasing use of global database methods in recent years, other study parameters were collected using various satellite sensors, based on satellite estimations. The relevant information is presented in Table 1.

Additionally, remote data, including solar UV radiation, relative humidity, cloud cover, and incoming shortwave flux of solar radiation, were gathered from https://giovanni.gsfc.nasa.gov/giovanni/

Considering that skin cancer data were on counties while other data were in pixel form, zonal statistics in the ArcGIS environment were utilized to calculate the mean for each parameter against each city. Additionally, due to the variations in values for different parameters, normalization was conducted to standardize values measured on different scales to a common scale between 0 and 1.

To determine the correlation between parameters influencing the incidence of skin cancer and the rate of skin cancer, the Pearson correlation coefficient was employed. Using the Pearson coefficient allowed for the identification of highly correlated parameters, which were subsequently omitted from the analysis.

Geostatistical analysis

For this study, where the spatial unit was a polygon, the Moran's I index was chosen due to its higher efficiency in assessing spatial autocorrelation for polygon-shaped data compared to other approaches [27]. After determining the spatial autocorrelation of the data, hot spot analysis (Getis-Ord Gi*) was applied to identify clusters, specifically hot and cold spots.

The Global Index of Spatial Autocorrelation (Moran's I)

The spatial distribution of any phenomenon, such as skin cancer, in a geographical space result in a distinct pattern that can be analyzed using Moran's index. The calculation of Moran's index involves the following steps:

$$I = \frac{n}{S_0} \frac{\sum_{i=1}^{n}\sum_{j=1}^{n} w_{i,j} z_i z_j}{\sum_{i=1}^{n} z_i^2} \quad (2)$$

Where Z_i is the difference between values of event i with an average of $(x_j - \bar{X}) w_{i,j}$ is the spatial weight between events i and j. n is the total number of events and S_0 is the sum of all spatial weights.

The total sum of the spatial weights is obtained using equation (3):

$$S_0 = \sum_{i=1}^{n}\sum_{i=1}^{n} w_{i,j} \quad (3)$$

The score of Z_i as a standard for the Moran statistic and can be calculated as shown below.

$$z_I = \frac{I - E[I]}{\sqrt{V[I]}} \qquad (4)$$

$$E[I] = -1/(n-1) \qquad (5)$$

$$V[I] = E[I^2] - E[I]^2 \qquad (6)$$

Hot Spot Analysis (Getis-Ord Gi*)

The Getis-Ord Gi hot spot analysis is formulated as follows:

$$G_i^* = \frac{\sum_{j=1}^{n} w_{i,j} x_j - \bar{X} \sum_{j=1}^{n} w_{i,j}}{s \sqrt{\frac{\left[n \sum_{j=1}^{n} w_{i,j}^2 - (\sum_{j=1}^{n} w_{i,j})^2 \right]}{n-1}}} \qquad (7)$$

where x_j is the attribute value for event j and w_{ij} is the spatial weight between events I and j. n shows the total number of events.

$$\bar{x} = \frac{\sum_{j=1}^{n} x_j}{n} \qquad (8)$$

$$s = \sqrt{\frac{\sum_{j=1}^{n} x_j^2}{n} - (\bar{X})^2} \qquad (9)$$

Geographical Weighted Regression (GWR)

Unlike global regression methods that apply the same relationship for all regions, GWR is a local method, which allows the regression relationship to vary across different regions [28]. This flexibility makes it superior to other regression approaches that assume a uniform relationship across the entire study area. Equation (10) formulates the geographical weighted regression method,

$$\beta(u) = (X^T W(u) X)^{-1} X^T W(u) Y \qquad (10)$$

where Y is the dependent variable at point u, X_j is the independent variable at point u, β are the model estimators, and W shows the square weight matrix and is dependent on the location of point u in the region. The weights are completely reliant on spatial location and the location of a point in relation to other points in the region.

Model Evaluation

After data preparation, geographical weighted regression was conducted using the data from 2022. The regression resulted in prediction maps for the prevalence of skin cancer. These prediction maps were then compared to the actual skin cancer rate maps to evaluate the performance of the geographical weighted regression. The determination coefficient (R^2) was used to assess the accuracy of the modeling process. A higher R^2 value implies a better fit of the model to the data, suggesting that the model captures a larger portion of the variation in the dependent variable based on the independent variables [29]. R^2 can be calculated using equation (11).

$$R^2 = \left(\frac{\sum_{i=1}^{n} (p_i - \bar{p})(o_i - \bar{o})}{n.s_{pred} s_{obs}} \right)^2 \qquad (11)$$

, where n is sample size, p_i is predicted disease rate, O_i is the observed disease rate, $\bar{p}$ shows the average predicted disease rates, $\bar{o}$ is the average observed disease rate, and S_{pred} is the standard deviation for the predicted disease rate and S_{obs} shows the standard deviation of disease rates between model input and output.

Limitations

In delineating the temporal scope of our study, the year 2022 was chosen as the baseline. This decision was grounded in the utilization of two primary data points: the overall population of Iran and the statistics pertaining to individuals with cancer within the Iranian population. In crafting this article, our reliance on the most accessible and up-to-date data was paramount. our dataset includes additional variables, such as the solar UV index (focused primarily on the UVB fraction), incoming shortwave flux, sunshine hours, cloud coverage rate, and relative humidity. It is crucial to note that these data represent averages. The comprehensive analysis of the "time evolution of the climate" typically necessitates a temporal span of at least 10 years and the application of intricate climatological models. Given the scale of our study, encompassing all synoptic stations across Iranian counties over a minimum 10-year period would be an extensive undertaking. Instead, we adopted a standardized method detailed in Table 1, wherein average values of the studied indices for the year 2022 were considered. While these averages retain the capacity to reflect the time evolution of the climate by capturing changes in climatic indices, it is essential to acknowledge that methodologically, they differ from analyses utilizing complex climatological models.

Further, it is crucial to emphasize that this study directly extracted climate change parameters from remote sensing output products, and as a result, no image processing was undertaken.

Results

Geographical distribution of climate change parameters

Figure (3-a) illustrates the annual average UV index map, a numerical representation of erythemal irradiance. The UV index is a dimensionless quantity proportional to the solar UV radiation spectrum, with a predominant focus on the UVB range (290-320 nm) and a smaller fraction in the UVA range (320-400 nm). This map reveals a clear north-south flow pattern in spatial changes of solar UV radiation, with a decrease from south to north. The numerical values of the UV index serve as indicators of potential health risks associated with sun exposure, with higher values corresponding to elevated UV radiation levels. The maximum UV radiation is observed in the south-eastern and central regions, highlighting areas with the highest UV index values. Similarly, the annual average of spatial changes for incoming shortwave flux (Fig. 3-b) exhibits a consistent pattern with the UV changes. This alignment underscores the influence of solar UV radiation, particularly in the UVB range, on overall shortwave flux variations. The UV index, by virtue of its calculation and representation, provides valuable insights into the geographical distribution of solar UV radiation and its

Michael Aryan Kya

Table 1. Data of the Study

Parameter	Time	Data source	Unit	Spatial Resolution
UV	2022 Annual average	OMI	UV Index	1°
Cloudiness	2022 Annual average	MODIS	%	1°
Incoming short-wave flux	2022 Annual average	MERRA-2	W m-2	0.5°*0.625°
Humidity	2022 Annual average	AIRS	%	1°
Elevation	2022	SRTM	Meter	90
Sunshine hours	2022	Niroo Research Institute	Hours	-

Figure 1. Steps Taken of the Study

Table 2. Statistical Description of the Parameters

Parameter/Statistic	Mean	MAX	Min
UV	7.74	8.61	6.54
Incoming shortwave flux	213	270	165
cloud	37.12	65.04	3.42
Relative humidity	14.22	37.18	0
Hours of Sunshine	3109	3567	1894
Digital Elevation Model (DEM)	2613	5593	-70

potential implications for human health.

The maximum value for incoming shortwave flux is also observed in the central and south-eastern regions.

Moving on to the spatial changes in total sunshine hours for 2022 (Fiure 3-c), the maximum value is observed in the central and eastern regions. This pattern can be attributed to the smaller latitude in these regions, as compared to the more complex topography in the northern areas when compared to the southern and central regions. Figure (3-d) displays the annual average spatial change in cloud coverage. The northern and north-western strips show the highest cloud coverage, while the southern and south-eastern strips have the minimum cloud coverage. Additionally, western regions generally have higher cloud coverage compared to eastern regions. Therefore, the cloud cover index follows both a north-south flow pattern and a west-east pattern. The spatial changes in relative humidity (Figure 3-e) indicate higher humidity in the

Table 3. Correlation Coefficient (R^2) of Influential Parameters with the Incidence Rate of Skin Cancer

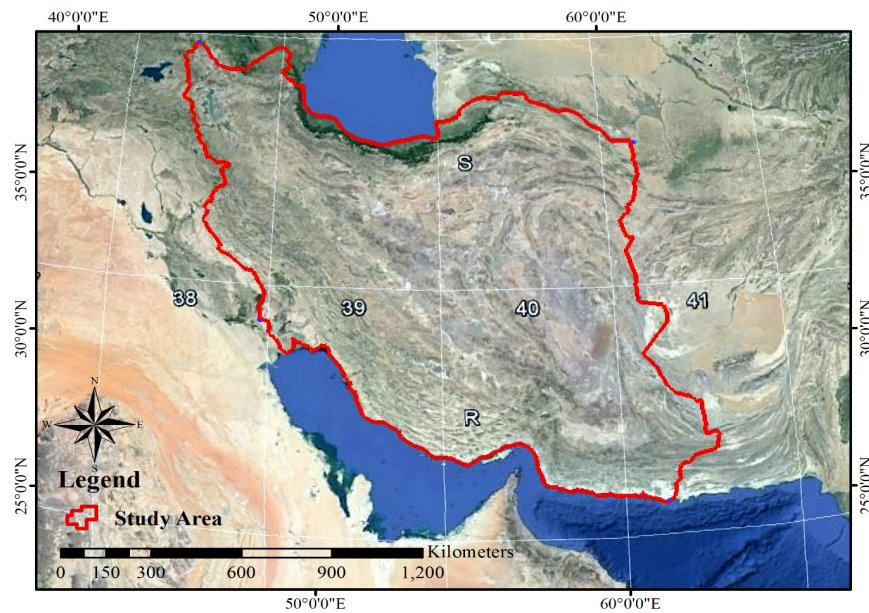| Parameter	UV	Relative humidity	Cloud coverage	Incoming shortwave flux	Sunshine hours	Altitude
The incidence rate of skin cancer	0.51	-0.43	-0.36	0.38	0.24	0.12

Figure 2. Area of Study. (Source: The data have been acquired from Google Earth the and the map have been created using of ArcGIS software)
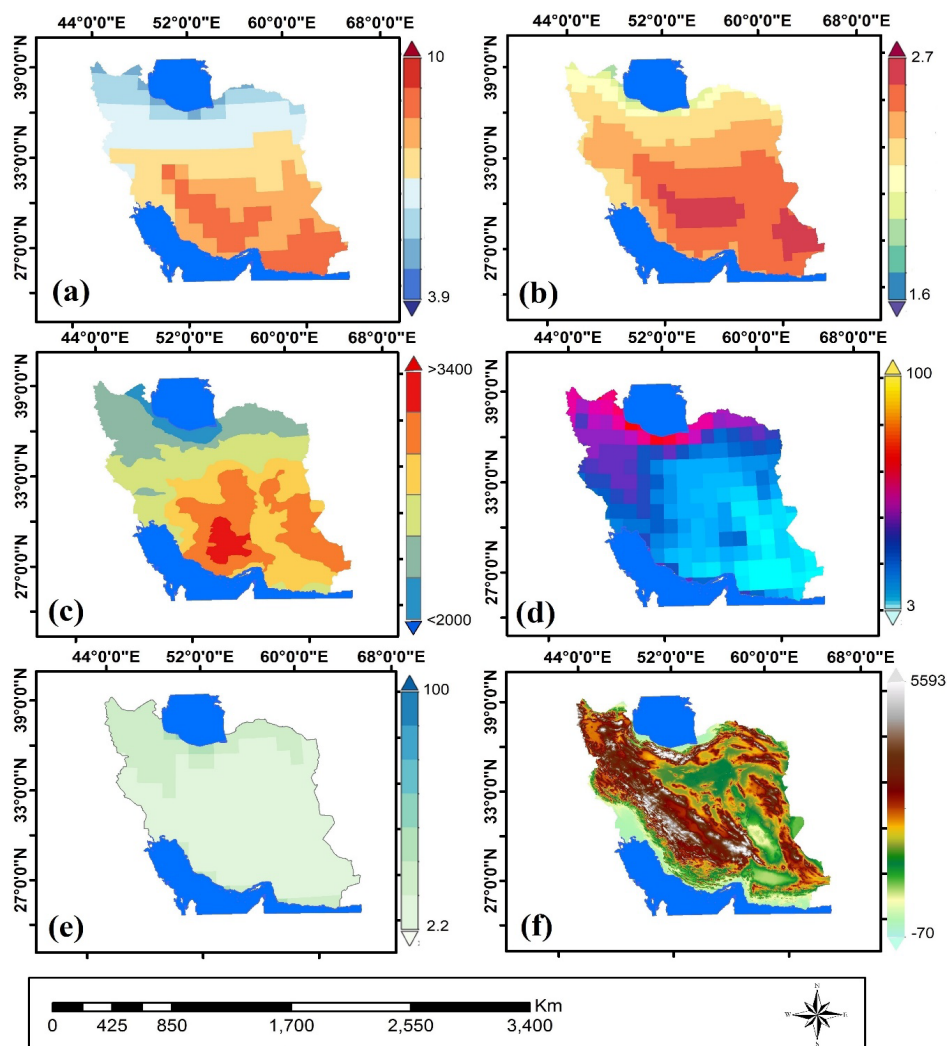

Figure 3. Influential Parameters in the Incidence of Skin Cancer. (a): Annual Average UV Index. (b): Annual Average Incoming Shortwave Flux. (c): Total Sunshine Hours Distribution. (d): Annual Average Cloud Coverage. (e): Relative Humidity Distribution. (f): Spatial Changes in Altitude. (Source: The data have been acquired directly from the NASA's EarthData 2022 and the maps have been created using of ArcGIS software).
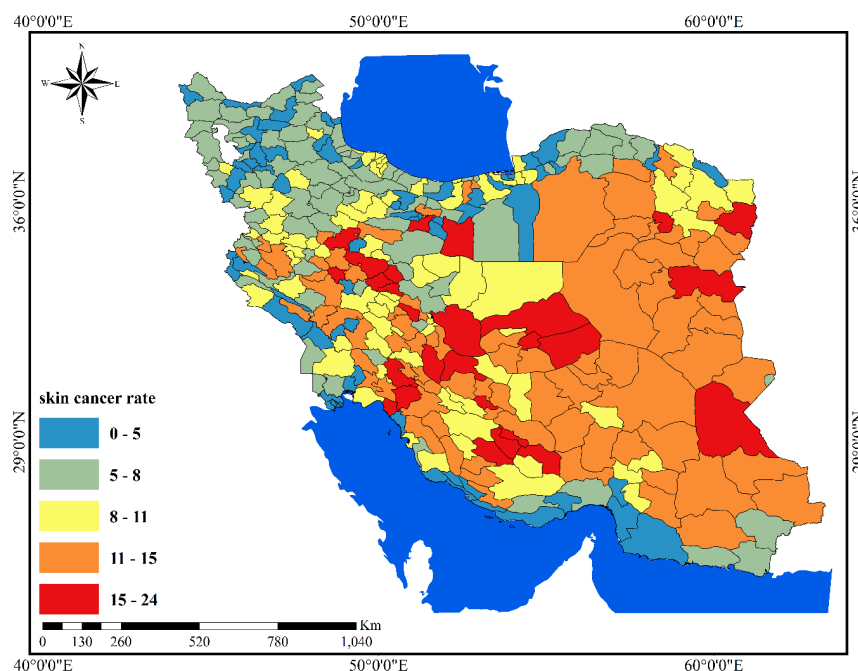
Figure 4. The Ratio of the Population Suffering from Skin Cancer

northern coastal regions, as well as both the north-western and north-eastern regions. Finally, Figure (3-f) illustrates the spatial changes in altitude. The Figure highlights a significant variation in altitude across the country, with western regions having higher altitudes compared to central and coastal regions.

Statistical analysis and correlation of data with skin cancer rates

A descriptive statistical analysis of the data proves useful in determining the range of different parameters in the study region. Table 2 provides the results of the descriptive statistical analysis of the collected data. It is evident that UV radiation in Iran varies between 6.54
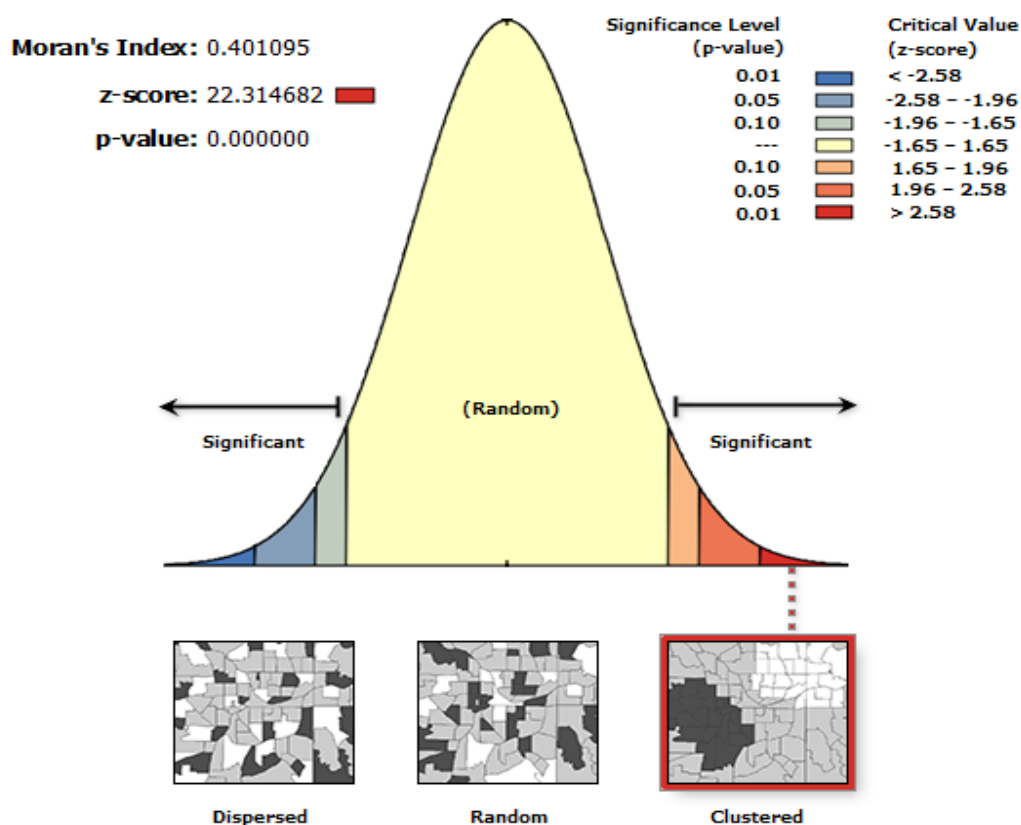

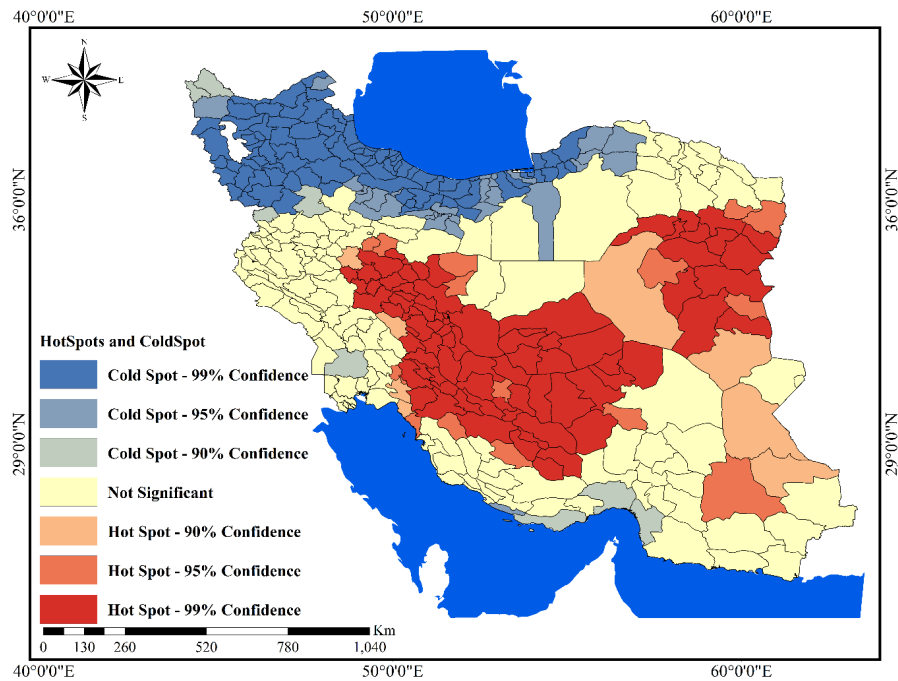
Figure 5. Moran's Index
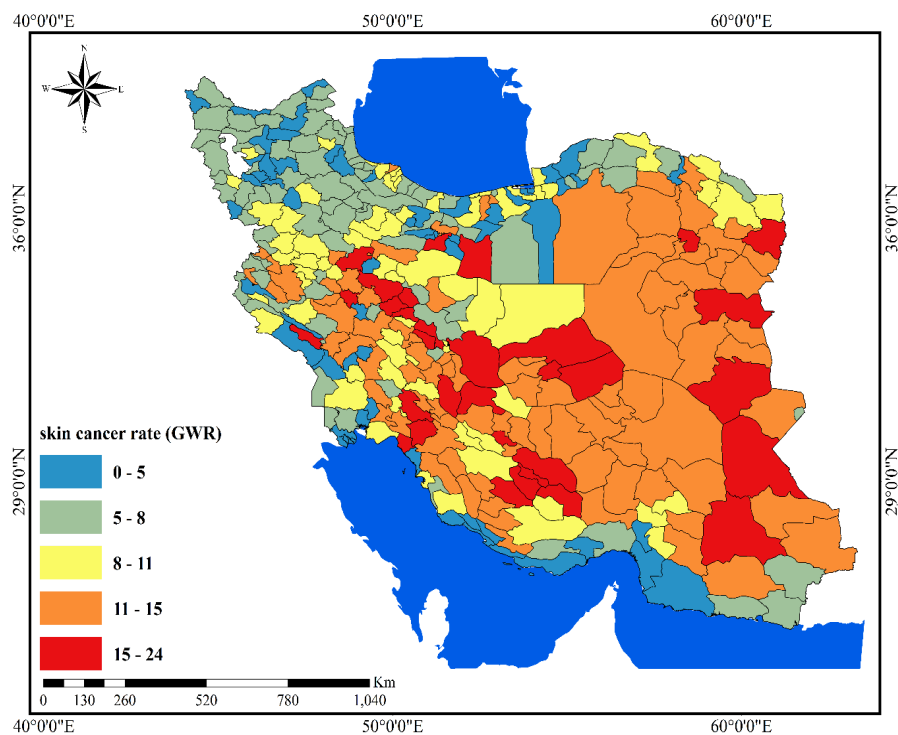
Figure 6. Hot and Cold Spots

Figure 7. The Modeled Map for the Incidence Rate of Skin Cancer

and 8.61, with the maximum value occurring in central regions. For incoming shortwave flux, values ranged from 1.65 to 2.7 W/m², showing a decrease as latitudes decreased. The percentage of humidity was between 0 and 37.18, which is relatively low due to Iran's arid and semi-arid climate. Cloud cover is another significant factor influencing skin cancer, with values ranging from 3.42% to 65.04%. Maximum cloud coverage was observed in the northern and southern coastal regions, while minimum values were found in central regions. The

DEM parameter, indicating the altitude, varied from -70 to 5593 meters, reflecting the high rate of altitude change within the country. Maximum altitudes were observed in the mountainous regions of Zagros and Alborz, whereas minimum altitudes were found in the coastal regions in the north of Iran.

Correlation analysis is indeed crucial in determining the relationships between different input parameters of a model. In this study, we investigated the correlation between various parameters, including UV radiation,

relative humidity, cloud coverage, incoming shortwave flux, altitude, sunshine hours, and the skin cancer rate. The correlation results are presented in Table 3.

The correlation coefficient between the mentioned parameters and skin cancer varied from -0.43 to 0.51, indicating a relatively moderate and downward correlation. The parameter with the highest positive correlation was UV, while relative humidity had the lowest negative correlation with the skin cancer rate. UV radiation, incoming shortwave flux, altitude, and sunshine hours showed a positive relationship with the skin cancer rate, whereas relative humidity and cloud coverage exhibited a negative relationship with this disease. The positive relation between altitude and skin cancer rate was observed; as altitudes increased, skin cancer rates also went up, although this correlation was exceptionally low. Considering that the observed correlations ranged from -0.43 to 0.51, we noted that correlations within the range of -0.67 to 0.49 have the potential to result in diverse outcomes for the mentioned parameters. The reason for this variability is that correlations closer to the extremes of this range indicate a stronger negative or positive relationship, which could significantly impact the modeling results. Given the sensitivity to correlation values within this range, it becomes imperative to include all parameters in the modeling process. This ensures a comprehensive consideration of the interconnected influences of the variables and enhances the robustness and reliability of the modeling outcomes.

After preparing the data and obtaining spatial maps containing addresses of residents diagnosed with skin cancer, the addresses were linked with the political division maps of the country, and further analytical processes were conducted based on the final maps. Additionally, a population map was obtained using demographic data from the Statistical Center of Iran. This population map was merged with the previous map indicating the number of residents suffering from skin cancer. Finally, utilizing equation 1, the skin cancer rate was calculated, and the results are presented in Figure 4.

As shown in Figure 4, the southeastern, southwestern, and central regions of Iran exhibit a higher rate of skin cancer compared to other regions. This is likely attributed to the elevated levels of UV radiation and sunshine hours, as well as the lower humidity prevalent in these areas.

Spatial autocorrelation and cluster patterns

Analysis were conducted in this study to examine the distribution of skin cancer. Initially, the spatial autocorrelation of skin cancer was assessed using Moran's I index, assuming a null hypothesis that the distribution of skin cancer was entirely random.

According to Figure 5, the Moran's I index was calculated to be 0.401095, with a p-value of zero and a z-score greater than 2.5. These results indicate that the skin cancer rate follows a clustered pattern. Thus, the null hypothesis, which assumes a random distribution of skin cancer, is rejected, and it is evident that the data are clustered. In other words, neighboring regions exhibit similar rates, forming clusters.

In the next stage, we conducted Getis-Ord Gi* to identify spatial clusters and regions associated with high skin cancer rates. As depicted in Figure 6, the analysis successfully identified clusters, hot spots, and cold spots. The results reveal that approximately 90 percent of the central regions of Iran are hot spots, showing statistically significant high rates of skin cancer. Conversely, the south-eastern and north-western areas of the country are identified as cold spots, indicating relatively lower rates. Consequently, the central area of Iran emerges as the primary focal point for skin cancer, with the rate decreasing as the distance from this central area increases, leading to the formation of cold spots.

Geographical Weighted Regression

After examining the spatial changes in skin cancer rates and performing geostatistical analysis, it was revealed that the distribution of skin cancer rates follows a clustered pattern, with specific regions marked as hot and cold spots across the country. Subsequently, an investigation into climate change variables demonstrated that skin cancer rates are influenced by changes in climate. This finding suggests that it is possible to model the spatial distribution of skin cancer using climate change parameters. To achieve this, geographical weighted regression with a comparative geographical core was utilized to model the skin cancer rate by considering relevant factors. The outcomes of this modeling process are presented in Figure 7.

Similar to Figure 4, Figure 7 also indicates that the highest skin cancer rates were observed in the central, southern, and south-eastern regions of Iran. A comparison between these two Figures reveals that the 0-5 and 15-24 level regions have decreased in the regression model map compared to the actual observation map. On the other hand, increases are evident in the 5-8 and 11-15 level regions. These differences are attributed to the varying effects of the parameters used in the modeling process. Moreover, upon comparing the two maps, it becomes apparent that skin cancer rates estimated by geographical weighted regression are higher for the north-western regions of the country compared to their actual values. This discrepancy may arise due to changes in altitude, atmospheric stability, and additional exposure to sunlight in those regions.

The R^2 value was relatively high ($R^2 = 0.71$) for the map modeled using geographical weighted regression in comparison to the actual map. This finding indicates that the skin cancer rate can be predicted fairly well using the effective variables introduced in this study.

Discussion

The results of the correlation between the effective parameters of skin cancer indicate a moderate initial relationship concerning the skin cancer rate. Consequently, focusing solely on one parameter and utilizing uni-variable regression is not sufficient for modeling purposes. Therefore, a multi-variable regression involving various parameters is necessary for effective modeling. Moreover, when comparing the results of this study with previous research, it is evident that the detection coefficient

obtained from the incidence rate and the modeled rate is reliable. The incorporation of remote sensing data and the consideration of spatial aspects can be identified as the main factors contributing to these outcomes.

Based on the statistical analysis conducted, both positive and negative signs taken into account, it was evident that relative humidity and UV radiation were identified as the most influential factors affecting the skin cancer rate. On the other hand, altitude was found to have the least impact on the skin cancer rate. Additionally, while examining the relationship and correlation between variables and skin cancer rate, the coefficients' signs for altitude, UV radiation, incoming shortwave flux, and sunshine hours indicated a direct relationship between these factors and the skin cancer rate. This implies that increases in altitude, UV radiation, incoming shortwave flux, and sunshine hours would lead to an increase in the skin cancer rate. Furthermore, the results of the geostatistical analysis revealed that the skin cancer rate exhibited a high spatial autocorrelation and was distributed in a clustered pattern. The spatial clusters with the highest probability of occurrence were concentrated in the central areas of the country.

The results obtained from GWR demonstrate that all the factors included in this study are effective in predicting the skin cancer rate. The findings from Figures 4 and 7 specify that the highest skin cancer rate was observed in the eastern, central, and southwestern regions of Iran. This is likely attributed to higher UV radiations and sunshine hours, as well as lower humidity and cloud coverage compared to other areas in the country. Even minor variations in latitude, along with the influence of high solar radiation resulting from the Azores high-pressure system in the atmosphere and clear skies, can have significant effects on skin cancer rates and contribute to the increase in the incidence of this disease.

The lowest rate of skin cancer was observed in the southern coastal regions of the Persian Gulf and the coastal regions of the Caspian Sea located in the northwest of Iran. This is likely attributed to higher relative humidity and cloud coverage in these areas, which effectively prevent direct exposure to sunlight. Additionally, as latitudes increase in the northern and northwestern coasts of Iran, solar rays change angles from vertical to oblique, resulting in lower skin cancer rates. The reduced sunshine hours in the northern regions of Iran also play a significant role in influencing the skin cancer rate.

As depicted in Figure 4, the southeastern, southwestern, and central regions of Iran exhibit a higher rate of skin cancer compared to other regions, aligning with findings in various international studies. In South Africa, the prevalence of skin cancer has shown a significant correlation with environmental factors such as solar ultraviolet radiation, ambient temperature, and rainfall [22]. Similarly, in Australia, a relationship has been found between temperature, humidity, ambient ultraviolet radiation, and UVR-related diseases such as cancer [30]. Furthermore, in the tropics, a study has indicated that environmental factors like solar ultraviolet radiation, air pollution, and variations in air temperature and relative humidity impact skin health [31].

The model validation of the GWR method revealed that when comparing the predicted map of the model with the actual map, the model exhibited a high coefficient of determination (0.71). This indicates that the geographical weighted regression model could account for approximately 71 percent of the data related to skin cancer rates.

In conclusion, the study aimed to leverage satellite data and GWR to generate predictive maps for the spatial distribution of skin cancer in Iran, with a specific focus on understanding the influence of climate changes. The utilization of remote sensing data was driven by several advantages, including the accessibility of digital and multi-spectral information, timely updates, a comprehensive overview of the study area, exploration across various electromagnetic spectra, repetitious coverage, and compatibility with various data formats. The datasets employed in this study encompassed crucial climate change factors, including UV radiation, relative humidity, cloud coverage, incoming shortwave flux, altitude, and sunshine hours. These diverse datasets facilitated a robust analysis of the spatial distribution of skin cancer in Iran and its intricate relationship with climate change factors. The key findings of this study underscore the significant influence of UV radiation and relative humidity on the skin cancer rate, with the former showing the highest positive correlation and the latter exhibiting the most substantial negative correlation. Furthermore, the geostatistical analysis unveiled a non-random, clustered spatial distribution of the skin cancer rate. The application of GWR demonstrated the high accuracy of the proposed model in predicting the skin cancer rate.

In addressing contradicting possibilities, it is essential to acknowledge the inherent complexity of the skin cancer phenomenon and recognize that other contributing factors may exist. Considering this, it is crucial to emphasize the need for ongoing research to further explore and refine our understanding of the multifaceted determinants of skin cancer. Regarding potential variables influencing the skin cancer rate beyond the climatic and altitude variables considered in this study, it is important to note that factors such as the duration of population exposure to outdoor environments, genetic predispositions, and skin phototype were not explicitly examined in the present work. Future investigations should encompass a broader spectrum of variables to comprehensively unravel the intricate interplay of factors contributing to skin cancer incidence. While this study provides valuable insights into the spatial distribution of skin cancer in Iran in the context of climate changes, it is imperative to acknowledge the complexity of the phenomenon and encourage continued research to address conflicting possibilities and explore additional variables that may contribute to our understanding of skin cancer dynamics.

Author Contribution Statement

Michael Aryan Kya

published version of the manuscript..

Acknowledgements

How the ethical issue was handled
Not required as data is not individualized, and there are no interventional in vivo tests.

Availability of data
Part of the datasets created and analyzed during this study are linked in the text. NASA and Google Earth data is achievable thorough the website. However, they can be obtained from the corresponding author upon request. Outcomes of the ArcGIS software is presented by the Figures.

Consent for publication
Author has given consent for publication.

Any conflict of interest
The author declares no potential conflict of interest.

References

1. Poniewierska-Baran A, Zadroga Ł, Danilyan E, Małkowska P, Niedźwiedzka-Rystwej P, Pawlik A. Microrna as a diagnostic tool, therapeutic target and potential biomarker in cutaneous malignant melanoma detection—narrative review. International Journal of Molecular Sciences. 2023;24(6):5386. https://doi.org/10.3390/ijms24065386.

2. Ogata D, Tsutsui K, Namikawa K, Moritani K, Nakama K, Jinnai S, et al. Treatment outcomes and prognostic factors in 47 patients with primary anorectal malignant melanoma in the immune therapy era. J Cancer Res Clin Oncol. 2023;149(2):749-55. https://doi.org/10.1007/s00432-022-03933-2.

3. De Fabo EC, Noonan FP, Fears T, Merlino G. Ultraviolet b but not ultraviolet a radiation initiates melanoma. Cancer Res. 2004;64(18):6372-6. https://doi.org/10.1158/0008-5472.CAN-04-1454.

4. Tucker MA, Goldstein AM. Melanoma etiology: Where are we? Oncogene. 2003;22(20):3042. https://doi.org/10.1038/sj.onc.1206444.

5. Vogel RI, Strayer LG, Engelman L, Nelson HH, Blaes AH, Anderson KE, et al. Sun exposure and protection behaviors among long-term melanoma survivors and population controls. Cancer Epidemiology and Prevention Biomarkers. 2017. https://doi.org/10.1158/1055-9965.EPI-16-0854.

6. Liu-Smith F, Ziogas A. An age-dependent interaction between sex and geographical uv index in melanoma risk. Journal of the American Academy of Dermatology. 2017. https://doi.org/10.1016/j.jaad.2017.11.049.

7. Apalla Z, Nashan D, Weller RB, Castellsague X. Skin cancer: Epidemiology, disease burden, pathophysiology, diagnosis, and therapeutic approaches. Dermatol Ther (Heidelb). 2017;7(Suppl 1):5-19. https://doi.org/10.1007/s13555-016-0165-y.

8. Salem HS. Cancer status in the occupied palestinian territories: Types; incidence; mortality; sex, age, and geography distribution; and possible causes. J Cancer Res Clin Oncol. 2023;149(8):5139-63. https://doi.org/10.1007/s00432-022-04430-2.

9. Rahouma M, Khairallah S, Dabsha A, Baudo M, El-Sayed Ahmed MM, Gambardella I, et al. Geographic variation in malignant cardiac tumors and their outcomes: Seer database analysis. Frontiers in Oncology. 2023;13:1071770. https://doi.org/10.3389/fonc.2023.1071770.

10. Weidner A, Kennedy R, Lamb C, Speight A, Rushton S, Thompson N. P50 is there evidence of geographical clustering of inflammatory bowel disease in newcastle upon tyne? BMJ Publishing Group. 2023. https://doi.org/10.1136/gutjnl-2023-BSG.122

11. Kiani B, Tabari P, Mohammadi A, Mostafavi SM, Moghadami M, Amini M, et al. Spatial epidemiology of skin cancer in iran: Separating sun-exposed and non-sun-exposed parts of the body. Arch Public Health. 2022;80(1):35. https://doi.org/10.1186/s13690-022-00798-2.

12. Iglesias-Puzas A, Conde-Taboada A, Aranegui-Arteaga B, Campos-Munoz L, Lopez-Bran E. Patients' characteristics and environmental factors affecting skin cancer detection: A multicentre prospective study. Acta Derm Venereol. 2023;103:adv11933. https://doi.org/10.2340/actadv.v103.11933.

13. Flynn MS, Cooper BR, Rundle CW, Anderson J, Laughter M, Presley CL, et al. Skin cancer, climate change, and opportunities for dermatologists. Curr Dermatol Rep. 2023:1-8. https://doi.org/10.1007/s13671-023-00390-z

14. Wheeler BW, Kothencz G, Pollard AS. Geography of non-melanoma skin cancer and ecological associations with environmental risk factors in england. Br J Cancer. 2013;109(1):235-41. https://doi.org/10.1038/bjc.2013.288.

15. Hu S, Sherman R, Arheart K, Kirsner RS. Predictors of neighborhood risk for late-stage melanoma: Addressing disparities through spatial analysis and area-based measures. J Invest Dermatol. 2014;134(4):937-45. https://doi.org/10.1038/jid.2013.465

16. Siddik MSM, Ahmed TE, Awad Ahmed FR, Mokhtar RA, Ali ES, Saeed RA. Development of health digital gis map for tuberculosis disease distribution analysis in sudan. J Healthc Eng. 2023;2023:6479187. https://doi.org/10.1155/2023/6479187.

17. Mazi PB, Sahrmann JM, Olsen MA, Coler-Reilly A, Rauseo AM, Pullen M, et al. The geographic distribution of dimorphic mycoses in the united states for the modern era. Clin Infect Dis. 2023;76(7):1295-301. https://doi.org/10.1093/cid/ciac882.

18. Pertuak AC, Latue P, Rakuasa H. Spatial approach in health predicting the spread of infectious disease incidence rates (malaria & covid-19) in ambon city, indonesia, a review. J Health Sci Med Ther. 2023;1(02):38-48. https://doi.org/10.59653/jhsmt.v1i02.234

19. Rajput NH. Mapping cancer in india: Implementing gis for cancer research and registries. Indian J Cancer.2023;60(3):293-4.

20. Isler MF, Coates SJ, Boos MD. Climate change, the cutaneous microbiome and skin disease: Implications for a warming world. Int J Dermatol. 2023;62(3):337-45. https://doi.org/10.1111/ijd.16297.

21. Baldermann C, Laschewski G, Grooss JU. Impact of climate change on non-communicable diseases caused by altered uv radiation. J Health Monit. 2023;8(Suppl 4):57-75. https://doi.org/10.25646/11653.

22. Wright CY, Norval M, Kapwata T, Du Preez DJ, Wernecke B, Tod BM, et al. The incidence of skin cancer in relation to climate change in south africa. Atmosphere. 2019;10(10):634. https://doi.org/10.3390/atmos10100634

23. Valavi EH, Rafie SH, Pakseresht PA, Siadat SI. Prevalence of skin cancer in southwest in Iran. Koomesh. 2013;15(1).

24. Rakhshan A, Moradi A, Masoudi E. Melanoma in iranian childhood and adolescence: An analysis of 14 patients.

Int J Cancer Manag. 2023;16(1). https://doi.org/10.5812/ijcm-121873

25. Balajam NZ, Mousavian A-H, Sheidaei A, Gohari K, Tavangar SM, Ghanbari-Motlagh A, et al. The 15-year national trends of endocrine cancers incidence among iranian men and women; 2005–2020. Sci Rep. 2023;13(1):7632. https://doi.org/ 10.1038/s41598-023-34155-2

26. Afzali M, Mirzaei M, Saadati H, Mazloomi-Mahmood-Abadi SS. Epidemiology of skin cancer and changes in its trends in iran. Feyz Med Sci J. 2013;17(5):505-11.

27. Black SR. User's Guide to planetary image analysis and geologic mapping in ArcGIS Pro. US Geological Survey; 2023.

28. Sun S, Zeng Z, Li Q. Exploring the visual distinguishability and topic autocorrelation of murals unearthed in china from the spatial perspective. J Inf Sci. 2023:01655515231202761.

29. Draper N, Smith H. Applied regression analysis: Wiley Interscience. New York. 1981.

30. Xiang F, Harrison S, Nowak M, Kimlin M, Van der Mei I, Neale RE, et al. Weekend personal ultraviolet radiation exposure in four cities in australia: Influence of temperature, humidity and ambient ultraviolet radiation. J Photochem Photobiol B. 2015;143:74-81. https://doi.org/10.1016/j.jphotobiol.2014.12.029.

31. de Paula Corrêa M, Marciano AG, Carvalho VSB, de Souza PMB, Ripper JdSC, Roy D, et al. Exposome extrinsic factors in the tropics: The need for skin protection beyond solar uv radiation. Sci Total Environ. 2021;782:146921.